IEEE Robotics and Automation Magazine (RAM) paper presented at
2024 IEEE/RSJ International Conference on Intelligent Robots and Systems (IROS)
October 14-18, 2024. Abu Dhabi, UAE

IEEE-RAM 23-0138

Variable Stiffness, Sensing, and Healing in FESTO's FinRay Gripper: An Industry-Driven Design

Seyedreza Kashef Tabrizian *Student member IEEE*, Seppe Terryn, Daniel Brauchle,
Jan Seyler, Joost Brancart, Guy Van Assche, Bram Vanderborght *Senior member IEEE*

***Abstract*— Soft grippers' rising popularity in industries is due to their impressive adaptability. Yet, this adaptability requires flexibility which often sacrifices grip firmness and complicates sensor integration. This paper introduces two additional innovations, variable stiffness and pneumatic sensing, into a FinRay adaptive gripper. The approach and design for incorporating these innovations are guided by requirements outlined by FESTO. Regarding this, a layer jamming-based variable stiffness skin broadens gripper applications, manipulating objects of varying hardness and weight, while a pneumatic sensor skin detects contact and loss of contact. Both functionalities rely on the airtightness of the skins, which is compromised if damaged. To address this, both the skins and the gripper were crafted using self-healing polymers. The sensing and modulated mechanical performance of the gripper were evaluated experimentally and through simulations, and the self-healing ability was assessed by recharacterization after a damage-healing. This work showcases the promising synergy between robotics and self-healing materials, demonstrating mutual reinforcement to a highly efficient gripping system.**

***Index Terms*—self-healing, adaptive grasping, variable stiffness, functional skin, sensing skin, FinRay effect**

I. INTRODUCTION

GRipping is the most widely applied use of soft robotics technology in the industry. Examples of companies that have ventured into this area include FESTO [1], and Soft Robotics [2]. However, there have also been companies that did not succeed and eventually ceased their activities [3]. In advanced gripping, adaptability to various hardness levels of different objects, the provision of sufficient force to pick up items, and sensory feedback are crucial. The first two features can be addressed by introducing a variable stiffness ability to the grippers [4], and the third one can be achieved by adding perception ability [5]. However, most industrial soft grippers lack variable stiffness and sensing capabilities [1], primarily due to the added complexity in design and processing, and concerns about their reliability.

Jamming-based variable stiffness mechanisms, such as granular jamming [3], and layer jamming [4], have been studied as promising solutions. One advantage of jamming mechanisms for industries is their activation by vacuum (pressure), which is a widely available source in most companies. FESTO, being a leading provider of pneumatic devices in the automation industry, is well positioned to leverage this advantage. However, FESTO is not interested in granular jamming due to concerns regarding punctures in the membrane that could lead to loss of the granules to the environment, potentially contaminating production lines. Additionally, in comparison to layer jamming, granular jamming necessitates the use of a filter to prevent the suction or escape of the grains.

Various sensory mechanisms have been explored in scientific literature to enhance the perception in soft robots, with electrical sensors being the most extensively studied [5]. However, this technology requires the use of electrically conductive materials, wiring, and often embedding the sensor within the main soft matter, complicating the manufacturing. Pneumatic sensing chambers [6], [7] present an alternative solution, offering a simple structure that includes a flexible chamber connected to a pressure sensor. When external contact occurs, the volume of the chamber is reduced, resulting in an increase in pressure. This technology enables to construct the sensor and finger from a single material in a one-step process. Moreover, it again aligns well with FESTO's products and main expertise, as it operates based on pneumatic principles.

Although both the layer jamming-based variable stiffness mechanisms and the pneumatic sensing chambers can be constructed using a variety of soft materials, employing self-healing (SH) materials with reversible bonds brings several advantages as follows [8], [9], [10]. One critical aspect is the requirement for an airtight chamber. Maintaining the integrity of the chamber poses a significant challenge as it can be punctured by external sharp objects. Finding a suitable material that possesses both high tear strength and the necessary mechanical properties for the primary function is not a straightforward task [3]. For layer jamming, high flexibility of the chamber is essential, while for the pneumatic sensing chamber, the material should be flexible and exhibit a fast elastic response. Another challenge arises when the material of the skin and the soft matter to which the skin is going to be attached are different. The connection between two dissimilar materials presents a significant challenge, as the interface relies on secondary, weak chemical interactions [11]. Using self-healing materials offer strong interfacial bonding in multi-material designs [11].

The FESTO FinRay-based tool is an adaptive finger, which is one of the two soft gripping tools of FESTO (together with the FESTO universal gripper) on the market (Fig. 1) [1]. Adaptation is crucial in grasping. Shape adaptation provides increased contact surfaces between the gripper and objects, reducing local forces and resulting in a more secure grasp. However, it is crucial to ensure that the structural stiffness of the gripper is not higher than the object it is gripping; otherwise, it could potentially cause damage to the object. In many cases, grippers conform to the shape of objects by gently pressing against them. The FESTO finger have challenges with handling delicate objects due to the stiffness of its material and structure [12]. Structural optimizations have been researched to tune the stiffness of FinRay grippers [13], [14], as well as introducing a two-state discrete variable stiffness through a snap-fit mechanism [15]. Although no external component needs to be added to the gripper with structural optimization, this approach has limitations in changing the stiffness, specifically in a controlled and continuous manner. Another solution to lower the structural stiffness is to make the gripper out of softer materials. However, this comes at the cost of low gripping force and can lead to grip failure. Therefore, there is a need to adjust the stiffness of the finger based on the manipulation task: a soft condition used for the gripping phase (delicate shape adaptability) and a stiff condition during the manipulation phase (to securely hold the object).

In addition, the finger lacks sensory information to detect contact and loss of contact. While the pneumatic parallel gripper, to which the fingers are attached, does have a position sensor, its current method of detecting grip failure is not reliable. When a grasp attempt fails, the gripper fully closes, indicating a potential issue with the grip. Nevertheless, due to the adaptability of the fingers, it's possible that the gripper closes fully even when there is an object securely held within its grasp. Furthermore, with only the position sensor, it can be challenging to differentiate between the actual point of grip failure and the point when the gripper intentionally releases the object. Moreover, there will be a lag in detecting the failure, as the gripper needs to close beyond a certain threshold before the failure can be detected. As such, equipping the adaptive finger with a contact detection sensor to provide information about the grip and the failure in grip is beneficial. The sensor can potentially be used to program the activation and deactivation of the variable stiffness mechanism too.

In this paper, previously developed Diels-Alder-based self-healing materials [8] are used to make the FESTO FinRay adaptive finger, equipped with the layer-jamming-based variable stiffness skin and the pneumatic sensing skin (Fig. 1). The two self-healing skins provide solutions for the variable stiffness and sensing challenges of the finger, respectively, as well as restoration of the airtightness after a puncture or cut. In addition, utilizing self-healing materials that are recyclable reduces environmental concerns related to the waste of polymeric materials in robotics applications [16]. The paper benchmarks two technologies that, in the authors' perspective, can be readily scaled up in response to industry demands. Additionally, this study examines the performance of Diels-Alder self-healing materials in real-world soft robotics applications, will show how the variable stiffness skin can compensate for the decreased firmness of the finger, necessary for a delicate shape adaptation and detrimental for the manipulation, due to the utilization of soft self-healing

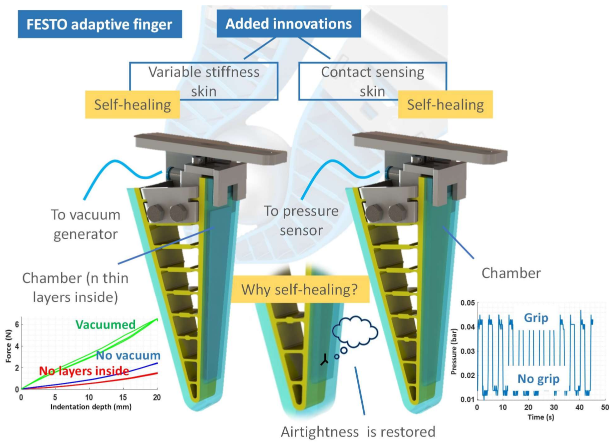

Fig. 1. FESTO adaptive finger equipped with a self-healing layer-jamming-based variable stiffness skin and pneumatic sensing skin. The healing ability allows it to restore airtightness after damage to the skin.

materials [16], and presents a comprehensive list of requirements necessary for the successful integration of self-healing materials into practical soft robotics systems. This can serve as a promising starting point for the commercialization of self-healing soft robots.

The methods employed in this study, including material selection, processing techniques, and characterization tools, are detailed in the next section. Afterwards, the results encompass the self-healing Fin-Ray finger, the layer-jamming based variable stiffness skin, and the sensing skin. Finally, the authors share their insights gained from the industrial collaboration in the discussion section.

II. MATERIALS AND METHODS

A. *FinRay-based adaptive finger with functional skins*

The biologist Leif Kniese drew inspiration from fish fins and developed the FinRay finger, which bears resemblance to the letter A in structure [13]. The FinRay finger features crossbeams positioned between the tip and base, as seen in Fig. 1. When external loads are applied to each side of the finger, it results in the deformation of the finger. FESTO provides three different finger sizes [17], and the middle size was chosen as the case study. The dimensions of the finger can be observed in Fig. 2. With the aim of benchmarking the performance of self-healing materials, the same design was adopted. To fabricate the skins, a 4 mm thick layer was applied to both sides of the finger (the greenish-blue color in Fig. 1 and Fig 2), incorporating a chamber on one side with a width of 2 mm, Fig. 2. The manual production became difficult when the chamber was smaller in size, and this also restricts the insertion of the layers for achieving the jamming effect. In the case of the sensing skin, the chamber was connected to a pressure sensor (SDET-22T-B2-G14-U-M12). On the other hand, for the variable stiffness skin, ten 0.2 mm thick sandpapers (P400) were inserted into the chamber (Fig 2), which was subsequently linked to a pressure source via a venturi-based vacuum generator (VN-07-M-I3-PQ2-VT2).

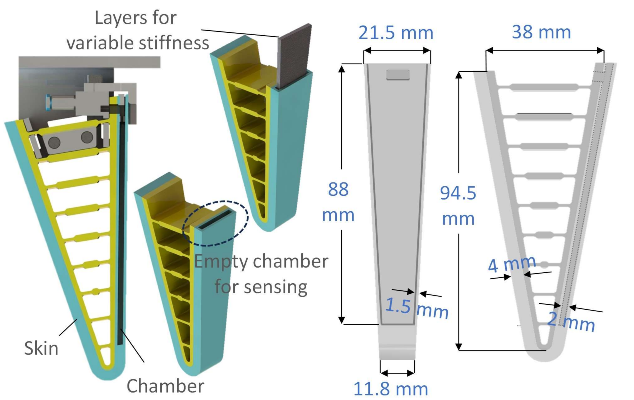

Fig. 2. Geometrical design of the FinRay adaptive finger, equipped with functional skins. The design of the chamber is the same for both skins.

Compared to rougher sandpapers, P400 sandpaper could be easily inserted and removed from the chamber, while less rough sandpapers could not provide enough friction for stiffness change upon vacuum. More information about the effect of friction and number of layers can be found at [18]. Apart from sandpaper, normal writing paper (twenty 0.1 mm layers) was also utilized for jamming, and the stiffness did not undergo noticeable changes upon vacuum. Section s1 (supplementary materials) provides the explanation of how the fingers are processed and how the cavities are made airtight.

In this study, the performance of the variable stiffness skin and the sensor skin was separately studied. However, it is interesting to establish a connection between these two components, where the contact is sensed by the sensor (shape adaptation phase of a grip), and then the variable stiffness skin becomes activated (manipulation phase of a grip).

B. *Selection of the self-healing materials*

The healing process of the material relies on Diels-Alder reactions between furan (diene) and maleimide (dienophile) (referring to supplementary materials section s2 and Fig. s2), forming reversible cross-links [8]. Thermoreversible Diels-Alder-based self-healing materials offer a broad range of mechanical properties, spanning from the kPa to GPa scale for their Young's modulus [8]. However, it is crucial to acknowledge that materials with high stiffness exhibit reduced molecular mobility and healing capability, as well as limitations in their fracture strain. In addition, the objective of reducing the structural stiffness of the FESTO adaptive finger acted as another constraint in material selection. On the other hand, highly soft materials compromise the finger's structural stability. Thus, DPBM F3000-r1 (hereafter referred to as “stiff material”) and DBPM F5000-r1 (hereafter referred to as “soft material”) were chosen to construct the finger. The mechanical and healing properties of these two materials are shown in Table 1. An initial evaluation through FEM simulation confirmed the functionality of these materials for the finger. To synthesize the materials and as opposed to the previous methodology [8], a new solvent-free method was employed, (supplementary materials section s3).

The chamber of the pneumatic sensing skin needs to possess both flexibility and a good elastic response. Consequently, the soft material exhibited the best performance for this particular application. However, for the chamber of the variable stiffness skin, the soft and stiff materials were not an appropriate selection. A softer chamber is advantageous to have an improved locking a result of the applied vacuum, as it can deform more easily. Therefore, DPBM F5000-r0.5 (hereafter referred to as “ultrasoft material”) was selected for the chamber of the variable stiffness skin (Table 1).

TABLE I. MECHANICAL AND HEALING PROPERTIES OF THE SELF-HEALING MATERIALS

Material	Young's mdl (MPa)	Fracture strain (%)	Fracture stress (MPa)	After damage-healing: Young's mdl (MPa)	After damage-healing: Fracture strain (%)	After damage-healing: Fracture stress (MPa)
DPBM-F3000-r1 (Stiff)	9.2	111.4	2.05	10.2	40.3	1.5
DPBM-F5000-r1 (Soft)	2.86	117.3	1.04	3.00	73	0.84
DPBM-F5000-r0.5 (Ultrasoft)	1.46	151.2	0.56	1.32	78.2	0.41

C. *Characterization methods*

For the self-healing fingers the following measurements were conducted:

- Indentation depth as a function of applied force via Zwick/Roell force measurement machine available at FESTO, headquarter (Fig. 3a). The experiment was conducted for both the pristine state of the fingers (both stiff and soft) and the damaged-healed state of the stiff finger. Consequently, the impact of the applied temperature required for healing was also investigated concerning the force exertion ability of the fingers. Considering the measuring point seen in Fig 3a, a 20 mm indentation depth was applied and the required force was measured.
- Endurance test via the test setup seen in Fig. 3b. It includes HGPL-14-40-A-B parallel grippers that opens and closes the fingers against a cylindrical rod (the diameter is 4 cm). This was done for both the pristine state and the damaged-healed state. The cycle numbers were recorded, where the first minor crack and the propagated ones were observed.
- Grasp success rate analysis via FESTO pneumatic cobot picking and placing 12 different objects ranging from 25 to 55 gr for four times (Fig. 3c). Each time, the objects were positioned in different locations.

  Comparison of the softness in shape-adaptation between self-healing and FESTO adaptive fingers by closing the fingers against four different soft bodies.

For the variable stiffness skin, the following measurements were conducted:

- Indentation depth as a function of applied force via Zwick/Roell force measurement machine (Fig 3a), (i) without 10 layers of sandpapers inside the chamber, (ii) with the layers but without vacuum, (iii) and with layers and vacuumed chamber.
- Airtightness test by measuring the vacuum inside the chamber before and after damage-healing.
- Grasp success rate analysis (Fig. 3c).
- Picking up a cylindrical object weighing 250 gr with and without vacuum.

For the pneumatic sensing skin, the following measurements were conducted:

- Using the test setup seen in Fig. 3b, the finger equipped with sensing skin closed and opened against the cylinder with four different frequencies (0.25, 0.5, 0.75, 1 Hz), while the pressure was recorded. This was done for both the pristine state and after damage-healing state.
- The previous test was conducted for half an hour to study the long-term performance with frequency of 0.75 Hz.
- Endurance test analysis (Fig. 3b), to see the effect of the chamber on the endurance of the finger. The result can be true for the variable stiffness sensing skin too.

III. Results

A. *Self-healing FinRay-based adaptive finger*

Evaluating the performance of self-healing materials for making the fingers is advantageous. In the case of a multilateral design for the skin and the finger, self-healing materials ensure a strong interfacial bonding between the skin and the finger [11]. Additionally, this can bring environmental benefits due to the recyclability of the materials. As such, the finger was constructed using self-healing materials as well. Both stiff and soft materials were used to construct the finger. The force required to bend the stiff finger (5.3 N at 20 mm indentation depth) was approximately 4.5 times higher than that needed to bend the soft finger (1.2 N at 20 mm indentation depth) (Fig. 4a). These measurements were repeated three times for reproducibility. Furthermore, the stiff finger was subjected to a healing study by the force measurement, to not only observe how the healing process works, but also to investigate the effect of temperature on the finger's performance (Fig. 4b). Three fingers were manually damaged on three different locations (Fig. 4b). The healing process for the stiff finger involved exposure to a temperature of 100-110 °C for 1 hour, followed by one day at room temperature. As depicted in Fig. 4b, there is a difference in the data between the pristine fingers and the healed ones. Observationally, no damage was seen in the healed fingers during the experiments. As a result, this difference is attributed to the fact that the Diels-Alder bonds are broken during heating and subsequently rebond upon cooling, which is the reason for the healing effect.

However, this reaction takes time, and one day at room temperature is not sufficient for all the broken bonds to fully rebond. It should be noted that the FESTO finger, according to the data sheet, exhibits a deformation force of approximately 20 N [17]. This indicates that the FESTO finger has a significantly higher resistance to bending compared to both the stiff and soft fingers mentioned earlier. A lower force required for deformation implies a more delicate shape adaptation, but it comes at the cost of providing less gripping force.

Fig. 4c illustrates the effect of bending stiffness on shape adaptation. In the case of a paper cup, the FESTO finger deformed it, whereas the soft and stiff self-healing fingers took the shape of the cup without any deformation Fig. 4c. Conversely, when dealing with a plastic cup, the stiff finger deformed it, while the soft finger delicately conformed to its shape (Fig. 4c). On the other hand, in the grasp success rate study (Fig. 3c) (supplementary video), the stiff finger achieved a success rate of over 90%, which was notably higher than

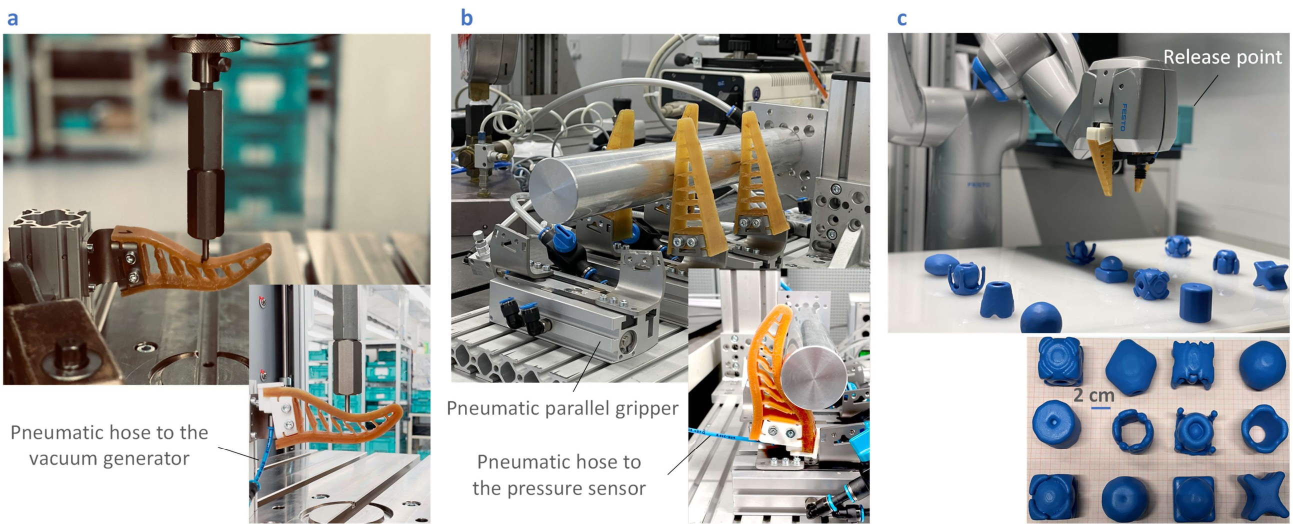

Fig. 3. Characterization. **(a)** Force measurement machine used for the fingers with and without the variable stiffness. **(b)** Test setup used for endurance analysis as well as for testing the sensor. **(c)** The pneumatic cobot used for the grasp analysis by picking and placing twelve different objects.

near 50% success rate achieved by the soft finger.

Apart from that, both fingers underwent an endurance test (Fig. 3b). The soft finger, with its material having a higher fracture strain (Table 1), demonstrated resistance to more than 7000 cycles before a minor crack with length of almost 1 mm was observed (Table 2). The crack was propagated to almost 80% of the length of the cross beam (counting from the bottom of the finger, the cross beam number 5 was more under strain in this test configuration (Fig. 2)) between 10000 to 12000 cycles. In contrast, the stiff finger showed signs of minor cracks before only 1000 cycles, which was propagated between 5000 to 6000 cycles (Table 2). The less endurance of the stiff finger can also be attributed to the higher stresses needed to deform the finger compared to the soft finger. In the event of damage, the fingers were healed and retested. The soft finger required 1 hour of exposure to a temperature of 90 °C, followed by one day at room temperature. After healing, the soft finger recovered its endurance properties, lasting almost the same number of cycles before any damage was observed (Table 2). However, the damage in the stiff finger appeared faster than the pristine state. Despite that, the propagation of the minor damages is not very fast in the FinRay design. It's worth noting that stiffer materials have less network mobility, necessitating a more substantial realignment of the damaged sides for effective healing. On the other hand, the soft material's higher network mobility allows it to fill microscopic gaps more easily upon heating, making precise realignment less critical. In addition, healing can be performed multiple times, resulting in a significant increase in longevity [8].

It is important to consider that the endurance test results are only valid for comparing the stiff and soft fingers that are made using the same production method for the fingers and synthesis strategy for the material, section s1 and s3 (supplementary materials) . However, enhancing production quality at an industrial level (one of the future tasks), and optimizing the geometry with the aim of extending the lifetime can have a substantial impact on the outcomes.

TABLE 2. ENDURANCE RESULTS OF THE SELF-HEALING FINGERS

Finger	Pristine		Healed	
	Minor rupture	Damage propagated	Minor rupture	Damage propagated
Stiff	C<1K	5K<C<6K	C<500	4K<C<5K
Soft	6K<C<7K	10K<C<12K	6K<C<7K	10K<C<12K

B. Variable stiffness skin

Based on the results of the soft and stiff finger (Fig. 4), it was evident that the soft finger exhibited more delicate shape adaptability (Fig. 4c), longer longevity (Table 2), and better

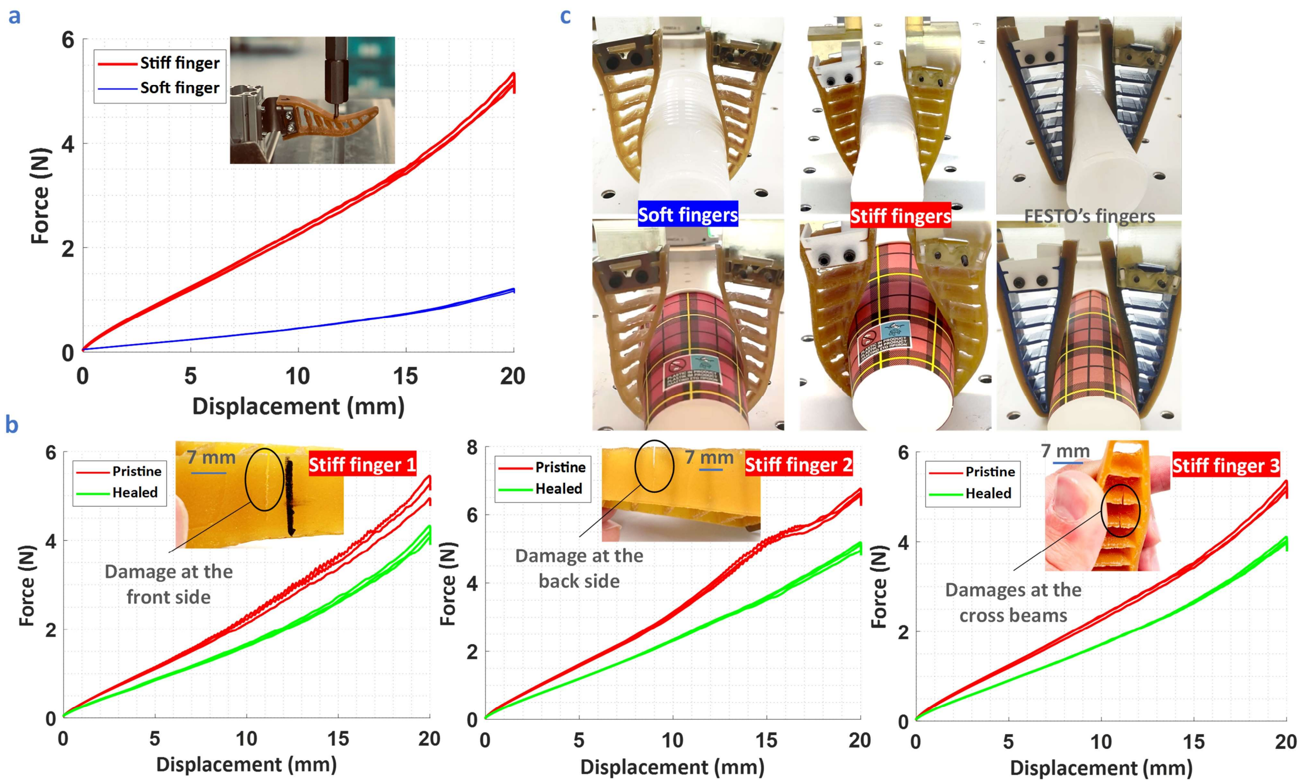

Fig. 4. Study of the soft and stiff self-healing fingers. **(a)** Indentation depth as a function of force. The stiff finger bends with 4.5 time more force compared to the soft finger. **(b)** Three stiff fingers were studied before and after damage-healing at different locations. The difference between the pristine and healed data is attributed to the effect of the healing temperature on the fingers, which makes them softer and requires more than one day to fully recover their properties. **(c)** The soft fingers delicately take the shape of the plastic and paper cup while the stiff fingers squeeze the plastic cup. The FESTO finger squeeze both of them.

healing ability (Table 1 and Table 2). However, one notable drawback was the relatively low grasp success rate of 40% (supplementary video). To leverage the advantages of the soft finger while addressing this issue, the layer-jamming-based variable stiffness skin was introduced. Fig. 5a illustrates the relationship between the supply pressure applied to the venturi-based vacuum generator and the generated vacuum inside the chamber. Notably, the maximum vacuum was achieved when the supply pressure was set to 7 bar. The chamber was severely damaged and then healed with the application of a thermal treatment at 90 °C for 1 hour, followed by remaining at room temperature for a day. As seen in Fig. 5b, it restored the airtightness, and the level of vacuum (with 7 bar supply pressure) remained the same before damage and after healing, and also stable in different cycles.

During the force measurement study, various vacuum pressures (relation with the supply pressure in Fig. 5a) were examined as well (Fig. 5c), repeating each test for three times. It was evident that up to an indentation depth of 15 mm, using a vacuum pressure of 0.72 bar (the supply pressure of 7 bar) resulted in higher bending stiffness. However, beyond 15 mm, all the graphs converged to a similar level. This phenomenon could be attributed to the slippage occurring between the layers, which is likely more prevalent before reaching a 15 mm indentation depth. It is essential to acknowledge that a higher vacuum does not necessarily guarantee a larger increase in stiffness. This outcome can vary based on external loads, the number of layers, and their frictional properties [4]. Considering the vacuum pressure of 0.72 bar (Fig. 5d), it was observed that activating the skin with the vacuum increased the bending force by approximately 2.75 times (Fig. 5d), from 2.4 N without vacuum to 6.6 N with vacuum. The FEM simulation result replicates the maximum force value, albeit with a trend that is not as linear as observed in the actual test (details are available in section s4 in the supplementary materials). The simulation focused solely on the layers and did not factor in the presence of the finger. Consequently, the variation in the trend could be attributed to the unmodeled interaction between the chamber and the layers. The force versus displacement behavior can be observed in the supplementary video, where both simulation and real footage are available for comparison. Moreover, the results indicated that the addition of layers inside the finger contributed to its bending stiffness, resulting in an increase in force from 1.5 N for the finger without layers to 2.4 N with layers inside (Fig. 5d). In contrast, the skin itself did not contribute significantly to the increase in bending stiffness, with the force going up from 1.3 N to 1.5 N when comparing Fig. 4a with Fig. 5c. In the grasp success rate study (Fig. 3c), the finger equipped with the variable stiffness skin demonstrated a success rate of over 95% in manipulating the 12 different objects, even without the application of the vacuum. This indicates that the increase in the finger's bending stiffness (the 2.5 N mentioned earlier) due to the layers inside was sufficient for the successful handling

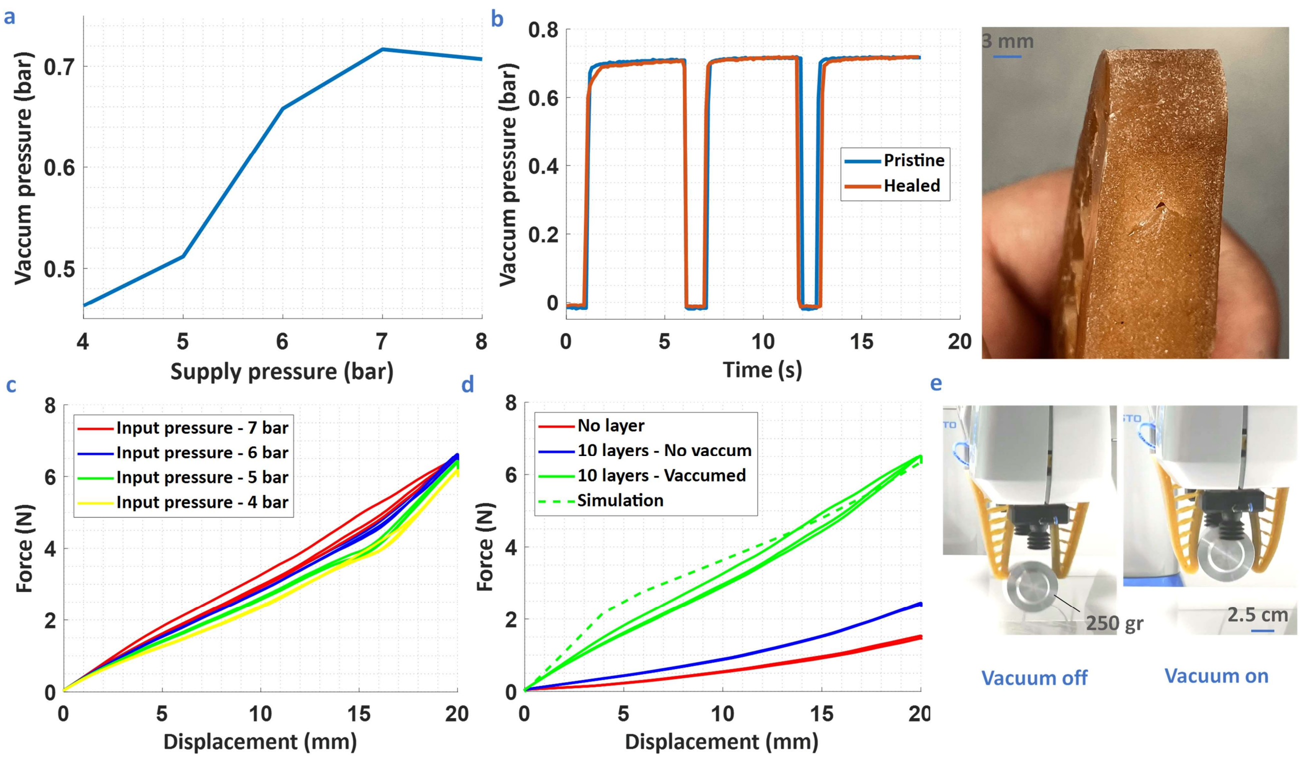

Fig. 5. Variable stiffness skin analysis. **(a)** The relation between the supply pressure to the vacuum generator and the resulted vacuum in the chamber. **(b)** Comparison between the vacuum inside the chamber before and after damage-healing. **(c)** The relation between force and indention depth at four different supply pressure of the vacuum generator. With 7 bar, more stiffness achieved, although after 15 mm of indention depth, all the graphs converged. **(d)** Comparison between the performance of the skin in three different states with supply pressure of 7 bar. The vacuumed state was also simulated by FEM in Abaqus **(e)** When the vacuum is applied, the fingers could pick up the object weighing 250 gr.

of those objects. Additionally, the softness of the skin's material (the ultrasoft one) could contribute to the improved grasping performance. As such and to benchmark the contribution of the variable stiffness skin, a cylindrical object weighing 250 grams was grasped and lifted up using the fingers. Throughout 9 trials, it was observed that with the vacuumed skin, the success rate was 100%, while without the vacuum, no successful picking was recorded (Fig. 5d) (supplementary video).

C. Pneumatic sensing skin

At FESTO, research on intelligent manipulation using AI algorithms is a prominent area of focus. However, this requires real-time data on object types and grasp conditions. One aspect is the detection of contact and loss of contact with objects. To provide a compatible solution with FESTO expertise and keeping the ease of production in mind, the self-healing pneumatic sensing skin was introduced, and the initial feasibility study was conducted. Using the test setup shown in Fig. 3b, a finger equipped with the sensing skin was closed and opened against the cylinder while measuring the pressure. In Fig. 6a, pressure values are observed at five different contact positions of the finger with the cylinder, ranging from the tip to the base of the finger. Moving towards the base, the trapezoidal shape of the chamber results in an increased volume being pressed. The greater the volume pressed, the more pronounced the change in the recorded pressure. This opens up the possibility to localize contact with objects and even to detect possible slippage when an object is being grasped. From this point forward, the sensor characterization was conducted at position 3, the same position used for endurance tests. Fig. 6b depicts the changes in pressure relative to the trajectory of the gripper during a cycle of opening and closing the finger against the cylinder at a frequency of 0.5 Hz. As seen, the change in pressure accurately corresponds to the gripper's state. Pressure increases when the gripper makes contact with the object, and decreases when the contact is released. The relation between contact position and pressure change is observed in the supplementary video, which presents the results of the FEM simulation as well as the real experiments. More details about the FEM simulation are available in supplementary materials section s5 . The pressure sensor exhibited an initial reading of 0.02 bar in its free state which was subtracted from the actual test values in Fig. 6.

This test was also performed at four different frequencies for 45 seconds, as well as after manually creating damage in the chamber and performing the healing (Fig. 7a-d). Although the change in pressure is relatively small, approximately 0.03 bar, the contact and loss of contact were clearly detected at all four frequencies (Fig. 7a-d). The similarity between the pristine data and the data after self-healing is evident, demonstrating the successful restoration of the skin's airtightness and recovery of the resulting sensing capabilities.

Furthermore, with the frequency of 0.75 Hz, the test was conducted for half an hour on the healed finger, and no drift in the data was observed (Fig. 7e). This result showcases the reliability and stability of the self-healing pneumatic sensing skin during extended use.

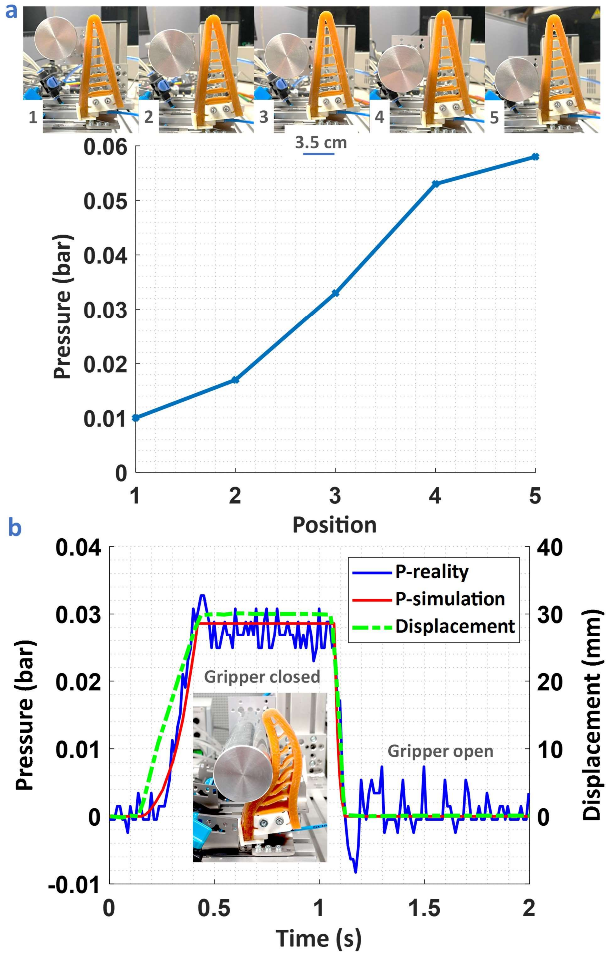

Fig. 6. Pressure changes in the pneumatic sensing skin. **(a)** The values of the pressure at five different contact positions show an increase in pressure changes with contacts closer to the base. **(b)** The relation between the position of the gripper with the change of the pressure inside the chamber at closing and opening frequency of 0.5 Hz.

Additionally, an endurance test, using the test setup in Fig. 3b, was performed on the soft finger equipped with the chamber of the sensing skin. After 12000 cycles, no damage was observed in the finger, whereas it was damaged at the connection to the mounting parts. This shows that, compared to the finger without the skin, the skin can act as a damping element during contact with external objects and reduces the impact.

However, the current design of the chamber for the sensing skin poses some limitations. It is essential to consider various object geometries to determine the limitations regarding the size of objects that the sensor skin can detect. For extremely small objects, the change in chamber volume could be too minimal to register a significant pressure variation. Additionally, the relative position of the grasped object in relation to the finger is another parameter that can impact the sensor's response (Fig. 6a). To increase the sensitivity, one potential solution could be to make the chamber in a convex shape relative to the finger, and even in a bi-stable manner.

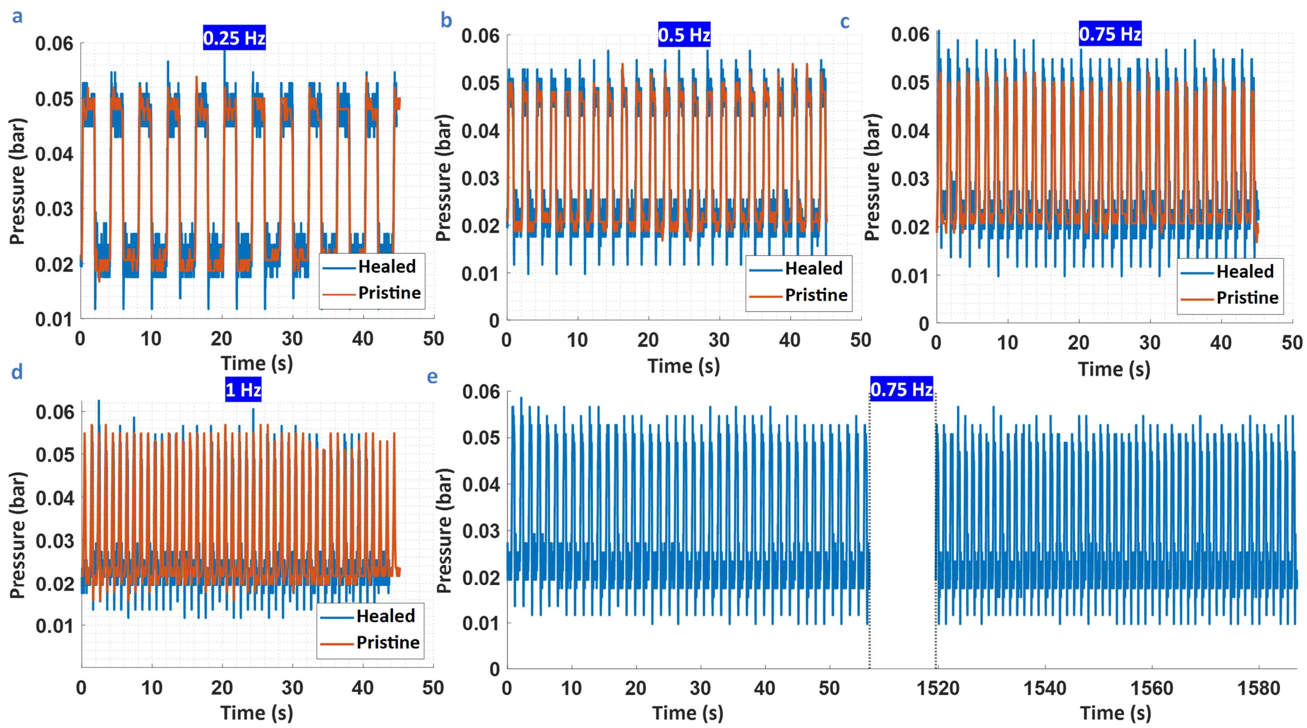

Fig. 7. Long-term performance of the sensing skin before and after damage-healing at four different frequencies of grasp, **(a)** 0.25 Hz **(b)** 0.5 Hz **(c)** 0.75 Hz **(d)** 1 Hz, for the closing and opening of the gripper. The sensor greatly shows the contact and loss of contact at all four frequencies, before and after damage-healing. **(e)** At frequency of 0.75 Hz, the test was conducted for half an hour, representing stability in the drift-free signal.

· V. DISCUSSION (SELF-HEALING MATERIALS IN ROBOTICS AND VICE VERSA)

As a response to the need raised to enable the FESTO adaptive finger to grasp delicate objects and provide feedback about the contact and loss of contact, two functional skins were introduced to the finger: the layer-jamming variable stiffness skin and the pneumatic sensing skin. The functionality of the skins relies on an airtight chamber, using the same design employed in this study. The distinction lies in the variable stiffness application, where ten thin sandpapers were inserted into the skin's chamber, while for sensing, the chamber remained empty. This shared design allows for transition between functions, switching from sensing to variable stiffness and vice versa. Nevertheless, different materials were utilized to fabricate the sensing skin and the variable stiffness skin. The chamber of the variable stiffness skin needs to be soft enough for easy suction, whereas the chamber of the sensing skin requires a fast elastic response. Depending on the application and grasp rate, it is entirely feasible to construct the chamber using a single material and alter its function based on the need. Another strategy involves the integration of both skins in a gripper, by arranging two chambers side by side, with the sensing chamber in direct contact with the objects. Upon detecting the grasp with the sensing skin and executing the shape adaptation phase of the grasp, the variable stiffness skin becomes activated, enabling more secure manipulation (see Fig. 8). To craft the gripper and the skins, Diels-Alder self-healing materials were used and evaluated to take one step further in utilizing the promising self-healing effect in soft robotics and approaching real industrial applications with them. However, it is worth mentioning that the functionality of the proposed skin does not rely on being self-healing. Depending on the applications, if the risk of damage to the gripper by objects is not high, non-self-healing materials can also be employed. As seen in Fig. 8, two grippers with both skins integrated are shown, where one is made of self-healing materials, and the other is made from dragon skin (supplementary materials section 6). Nevertheless, the use of self-healing materials offers the following contributions:

- Both skins require airtightness in their function. In the case of damage, the function is lost. The self-healing chamber can restore the airtightness to recover the function, thus increasing the lifetime of the product, which is a crucial industrial requirement.
- The reversible chemistry that provides self-healing, also provides great bonding in multilateral designs, alleviating concerns about debonding at the interface of the skin and the finger in case they are made out of two materials [11]. Although the FinRay-based finger is less sensitive to damage, multilateral bonding is one more reason why fabricating the finger out of self-healing materials is beneficial.
- The recyclability of the materials offers significant environmental advantages, particularly when large-scale implementation is a matter of concern [16].

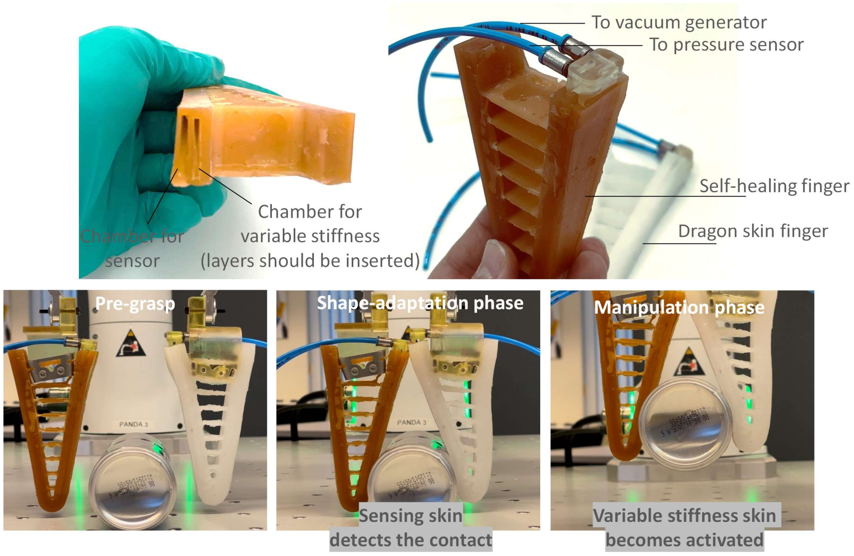

Fig. 8. The concept of combining both sensing and variable stiffness skins in a gripper. In this configuration, the sensing skin can detect contact during the shape adaptation phase of the grasp. During this phase, the variable stiffness skin is not activated, resulting in a softer structure and more delicate shape adaptation. Subsequently, the variable stiffness is activated for a more secure manipulation.

However, there are few issues with integrating the self-healing materials for gripping applications, which the variable stiffness skin could address as follows:

- In the case of using a soft material for the finger, the variable stiffness mechanism compensates for the lower gripping force of the finger. This enables the use of softer materials for the finger which has the following advantages as well: (i) Generally speaking, softer materials exhibit higher healing capabilities due to higher network mobility. Click or tap here to enter text.(ii) Softer materials have higher fracture strain properties that extend the functional lifetime of the system.
- When the finger and the skin are heated up for healing, it takes time for the finger to fully recover its force exertion ability. The variable stiffness skin makes it possible to faster bring the fingers to the operational state, as it actively compensates for the force.

Additionally, there are still other parameters that need to be characterized for the developed self-healing functional skin-equipped fingers to progress towards commercialization. These include, but are not limited to, further measurements of the lateral force and retention force of the fingers, as well as measuring the out-of-plane deformation.

Regarding the self-healing materials, several areas for research exist to better meet the requirements for industrial robotics applications:

- The necessity of elevated temperatures for the healing process introduces certain challenges for users, particularly in relation to infrastructure and cost. Therefore, room-temperature healing materials are a favorable option [19]. However, in general, room-temperature healing may not offer mechanically stable materials. An alternative approach could involve the integration of heating systems for controlled, localized healing activation [20], although this introduces additional complexity to the systems.
- As time is of utmost importance in industries, achieving fast healing is crucial [21].
- In the processing stage, fast curing time is also of paramount importance.
- Realignment of the damaged sides is crucial for effective healing, but not all customers may be able to perform it proficiently. Setting appropriate expectations for customers, such as highlighting that the self-healing process is more effective for smaller holes, becomes essential as this physical healing constraint can significantly impact efficiency. An alternative method may consist of incorporating damage closure systems [22], albeit at the cost of introducing added complexity to the existing systems.
- High toughness is crucial to prevent material fractures. However, the developed Diels-Alder self-healing materials have lower toughness than the FESTO material used for the finger. Although the design, processing, and material were not optimized for endurance analysis, minor damages were observed in the soft self-healing finger after 7000 grip cycles. This is not an industrially accepted value. Further study on the material properties can noticeably improve the endurance. Alternatively, self-healing materials can only be used for skins, with the finger made from other suitable materials, but a strong connection between the two materials must be established.

ACKNOWLEDGMENT

This work has received funding from the European Union's Horizon 2020 research and innovation programme under the Marie Sklodowska-Curie grant agreement No 860108 (SMART), as well as the SHINTO project which is funded under the European Innovation Council (EIC) programme of the European Union with grant agreement ID of 101057960. The authors gratefully acknowledge the Fonds Wetenschappelijk Onderzoek (FWO) for the personal grants of S. Terryn (1100416N) and J. Brancart (12E1123N).

The first author would like to acknowledge the generous support and resources provided by FESTO headquarters located in Esslingen, Germany, for the research stay that enabled most of this study to be conducted. In addition, the support of Rolf Mueller in the force measurement study and providing the test setup for endurance analysis is highly appreciated.

References

[1] B. Zhang, Y. Xie, J. Zhou, K. Wang, and Z. Zhang, "State-of-the-art robotic grippers, grasping and control strategies, as well as their applications in agricultural robots: A review," *Computers and Electronics in Agriculture*, vol. 177. Elsevier B.V., Oct. 01, 2020. doi: 10.1016/j.compag.2020.105694.

[2] Soft Robotics, "Robot Advancements Drive Efficiency, Productivity in Protein Processing." Accessed: Jul. 06, 2023. [Online]. Available: https://info.softroboticsinc.com/robot-advancements-drive-efficiency-productivity-in-protein-processing

[3] J. Amend, N. Cheng, S. Fakhouri, and B. Culley, "Soft Robotics Commercialization: Jamming Grippers from Research to Product," *Soft Robot*, vol. 3, no. 4, pp. 213–222, Dec. 2016, doi: 10.1089/soro.2016.0021.

[4] Y. S. Narang, J. J. Vlassak, and R. D. Howe, "Supp. Mechanically Versatile Soft Machines through Laminar Jamming," *Adv Funct Mater*, vol. 28, no. 17, Apr. 2018, doi: 10.1002/adfm.201707136.

[5] H. Wang, M. Totaro, and L. Beccai, "Toward Perceptive Soft Robots: Progress and Challenges," *Advanced Science*, vol. 5, no. 9, 2018, doi: 10.1002/advs.201800541.

[6] H. Yang, Y. Chen, Y. Sun, and L. Hao, "A novel pneumatic soft sensor for measuring contact force and curvature of a soft gripper," *Sens Actuators A Phys*, vol. 266, pp. 318–327, Oct. 2017, doi: 10.1016/j.sna.2017.09.040.

[7] C. Tawk, M. in het Panhuis, G. M. Spinks, and G. Alici, "Soft Pneumatic Sensing Chambers for Generic and Interactive Human–Machine Interfaces," *Advanced Intelligent Systems*, vol. 1, no. 1, p. 1900002, May 2019, doi: 10.1002/aisy.201900002.

[8] S. Terryn, J. Brancart, D. Lefeber, G. Van Assche, and B. Vanderborght, "Self-healing soft pneumatic robots," *Sci. Robot.*, vol. 2, no. 9, pp. 1–13, 2017, doi: 10.1126/scirobotics.aan4268.

[9] A. Pena-Francesch, H. Jung, M. C. Demirel, and M. Sitti, "Biosynthetic self-healing materials for soft machines," *Nat Mater*, vol. 19, no. 11, pp. 1230–1235, Nov. 2020, doi: 10.1038/s41563-020-0736-2.

[10] V. Kumar, U. H. Ko, Y. Zhou, J. Hoque, G. Arya, and S. Varghese, "Microengineered Materials with Self-Healing Features for Soft Robotics," *Adv. Intell. Syst.*, vol. 3, no. 7, p. 2100005, Jul. 2021, doi: 10.1002/aisy.202100005.

[11] S. Terryn, E. Roels, J. Brancart, G. Van Assche, and B. Vanderborght, "Self-healing and high interfacial strength in multi-material soft pneumatic robots via reversible diels-alder bonds," *Actuators*, vol. 9, no. 2, pp. 1–17, 2020, doi: 10.3390/ACT9020034.

[12] G. Schouterden, R. Verbiest, E. Demeester, and K. Kellens, "Robotic cultivation of pome fruit: A benchmark study of manipulation tools—from research to industrial standards," *Agronomy*, vol. 11, no. 10, Oct. 2021, doi: 10.3390/agronomy11101922.

[13] W. Crooks, G. Vukasin, M. O'Sullivan, W. Messner, and C. Rogers, "Fin Ray® effect inspired soft robotic gripper: From the robosoft grand challenge toward optimization," *Frontiers Robotics AI*, vol. 3, no. NOV, Nov. 2016, doi: 10.3389/frobt.2016.00070.

[14] P. Manoonpong *et al.*, "Fin Ray Crossbeam Angles for Efficient Foot Design for Energy-Efficient Robot Locomotion," *Adv. Intell. Syst.*, vol. 4, no. 1, p. 2100133, Jan. 2022, doi: 10.1002/aisy.202100133.

[15] J. Bastien and L. Birglen, "Variable Stiffness Soft Robotic Fingers Using Snap-Fit Kinematic Reconfiguration," *IEEE Transactions on Robotics*, vol. 39, no. 6, Dec. 2023, doi: 10.1109/TRO.2023.3303850.

[16] S. Terryn *et al.*, "A review on self-healing polymers for soft robotics," *Mater. Today*, vol. 47, no. xx, pp. 187–205, 2021, doi: 10.1016/j.mattod.2021.01.009.

[17] "Adaptive gripper fingers DHAS." Available: https://www.festo.com/media/pim/048/D15000100122048.PDF

[18] M. Ibrahimi, L. Paternò, L. Ricotti, and A. Menciassi, "A layer jamming actuator for tunable stiffness and shape-changing devices," *Soft Robot*, vol. 8, no. 1, pp. 85–96, 2021, doi: 10.1089/soro.2019.0182.

[19] S. Terryn, J. Brancart, E. Roels, G. Van Assche, and B. Vanderborght, "Room Temperature Self-Healing in Soft Pneumatic Robotics," *IEEE Robot Autom Mag*, vol. 27, no. 4, pp. 44–55, 2020.

[20] S. Kashef Tabrizian *et al.*, "A Healable Resistive Heater as a Stimuli-Providing System in Self-Healing Soft Robots," *IEEE Robot. Autom. Lett.*, vol. 7, no. 2, pp. 4574–4581, 2022, doi: 10.1109/LRA.2022.3150033.

[21] A. Safaei *et al.*, "Fast Self-Healing at Room Temperature in Diels-Alder Elastomers," *MDPI Polymers*, vol. 15, no. 17, 2023, doi: 10.3390/polym15173527.

[22] S. Kashef Tabrizian *et al.*, "Assisted damage closure and healing in soft robots by shape memory alloy wires," *Sci Rep*, vol. 13, no. 1, Dec. 2023, doi: 10.1038/s41598-023-35943-6.

Seyedreza Kashef Tabrizian, Vrije Universiteit Brussel and imec, Brussels, Belgium. Email: seyedreza.kashef.tabrizian@vub.be.

Seppe Terryn, Vrije Universiteit Brussel and imec, Brussels, Belgium. Email: seppe.terryn@vub.be.

Daniel Brauchle, FESTO Headquarters, Esslingen, Germany. Email: daniel.brauchle@festo.com.

Jan Seyler, FESTO Headquarters, Esslingen, Germany. Email: jan.seyler@festo.com.

Joost Brancart, Vrije Universiteit Brussel, Brussels, Belgium. Email: joost.brancart@vub.be.

Guy Van Assche, Vrije Universiteit Brussel, Brussels, Belgium. Email: guy.van.assche@vub.be.

Bram Vanderborght, Vrije Universiteit Brussel and imec, Brussels, Belgium. Email: bram.vanderborght@vub.be.